Supplemental Information
Photocatalytic CO_2 Reduction by H_2O: Insights from Modeling Electronically Relaxed Mechanisms

Samiksha Poudyal, Siris Laursen*

Department of Chemical and Bimolecular Engineering, University of Tennessee, Knoxville, TN 37996

Contents

Email address: `slaursen@utk.edu` (Siris Laursen*)

Preprint submitted to Catalysis Science & Technology *January 19, 2019*

1. Method Section (Continued)

1.1. Determination of the surface termination

To determine the surface termination of SiC and GaN, an ab initio approach was utilized [1, 2]. We calculated Gibbs free energies of surfaces in three different scenarios to isolate the surface termination under reaction conditions(reaction at 350 °C, 90 mol% H_2O at 1 atm pressure). For the first case, stoichiometric non-metal rich surfaces were modeled to reflect the surfaces from freshly cut bulk or surfaces closest to when they are first introduced to the reaction environment. In the second case, non-metal atom lean surface was produced by removing N or C atoms one by one from GaN or SiC surfaces by reacting with H from H_2O to produce balance CH_4 and O_2 or NH_3 and O_2 until the surfaces were completely metal rich. In the third case, surfaces were loaded with additional non-metal atoms to manually produce a non-metal rich surface. The stability of surface was determined at a point where the thermodynamics of removing an atom from the surface sequentially changed from endothermic to exothermic. Assuming a flow reactor regime where products formed would be continuously swept away from the catalyst surface, the chemical potentials of the products – CH_4, NH_3, and O_2 were assumed to be negligible. This resulted in the calculations only dependent on the chemical potential of H_2O and formation energies of NH_3 or CH_4 and O_2. Ab initio calculation results are presented below in Figure S1. Results indicate that both stoichiometric SiC and GaN are in fact lowest energy surfaces.

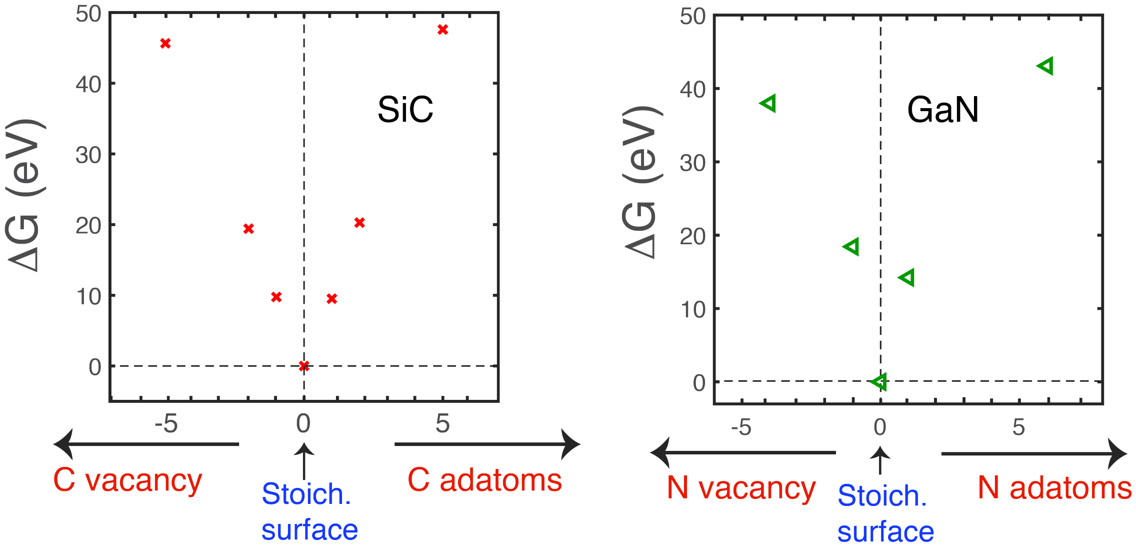

Figure S1: Ab initio thermodynamic energetics were utilized to isolate the surface termination of (left) SiC and (right) GaN. Gibbs free energies were calculated by taking hydrogenated C (CH_4) and N (NH_3) as references for atoms added or removed from the surfaces of SiC and GaN, respectively. Results suggested that stoichiometric surfaces are most stable in both cases.

1.2. Entropy Calculation

To determine the entropy change of the reaction steps such as H_2 evolution over GaN versus hydrogenation of CH* to CH_2 over SiC, vibrational frequencies (in cm^{-1}) were calculated using DFT. The vibrational contribution is calculated from frequencies in harmonic approximations:

$$S_{vib} = \sum_i h\nu_i/kT[exp(h\nu_i/kT) - 1]^{-1} - ln[1 - exp(-h\nu_i/kT)] \tag{1}$$

where, h is Planck's constant, ν is calculated wavenumbers from DFT (cm^{-1}), c is speed of light, k is Boltzman constant, and T is temperature (350 °C).

2. Model Figures

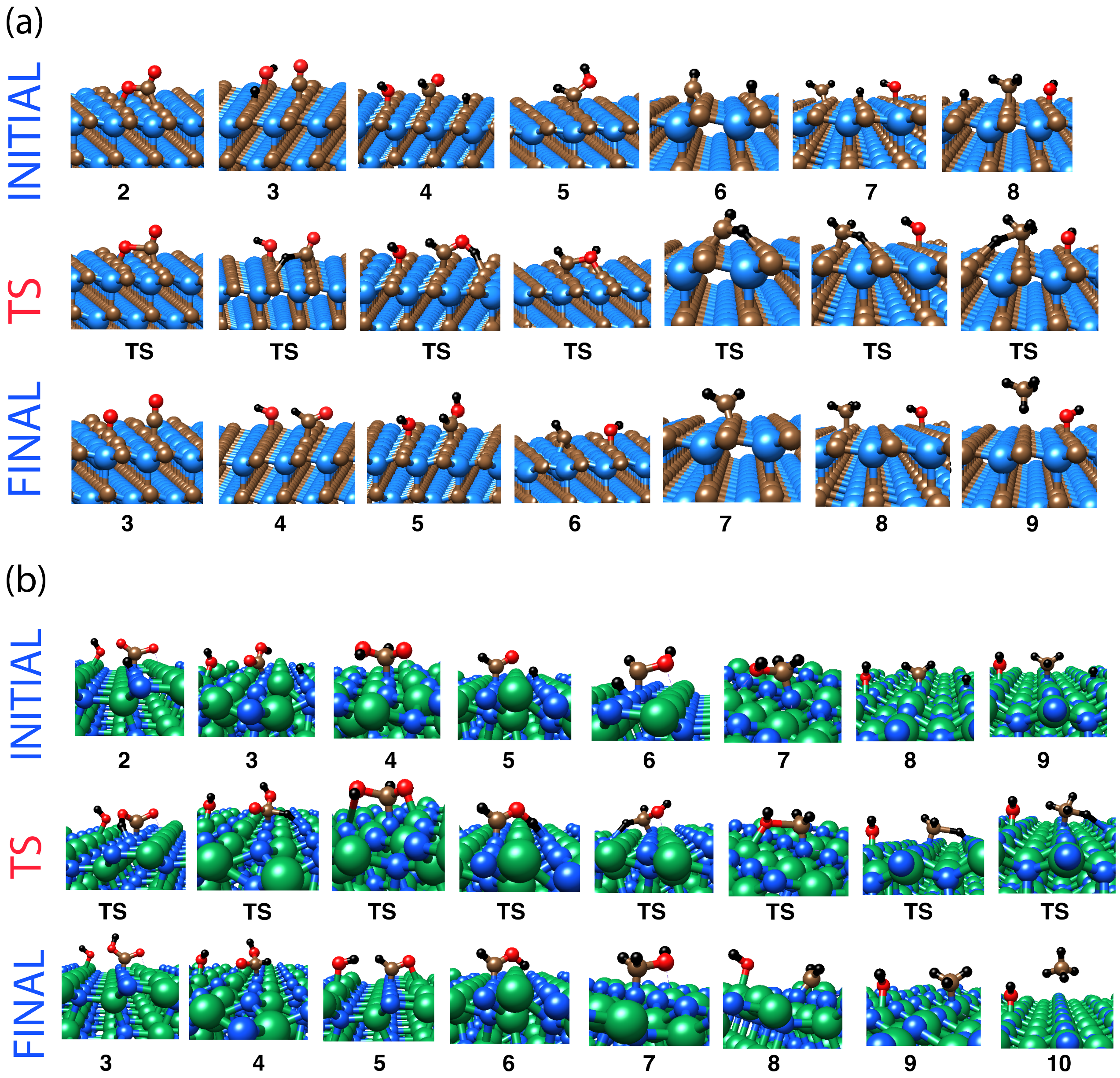

Figure S2: Model figures of most thermodynamically favorable reaction pathways over (a) SiC and (b) GaN: (top) initial step, (center) transition state, and (bottom) final step

3. Calculation Results

3.1. Most Favorable reaction energetics with stoichiometrically balanced species

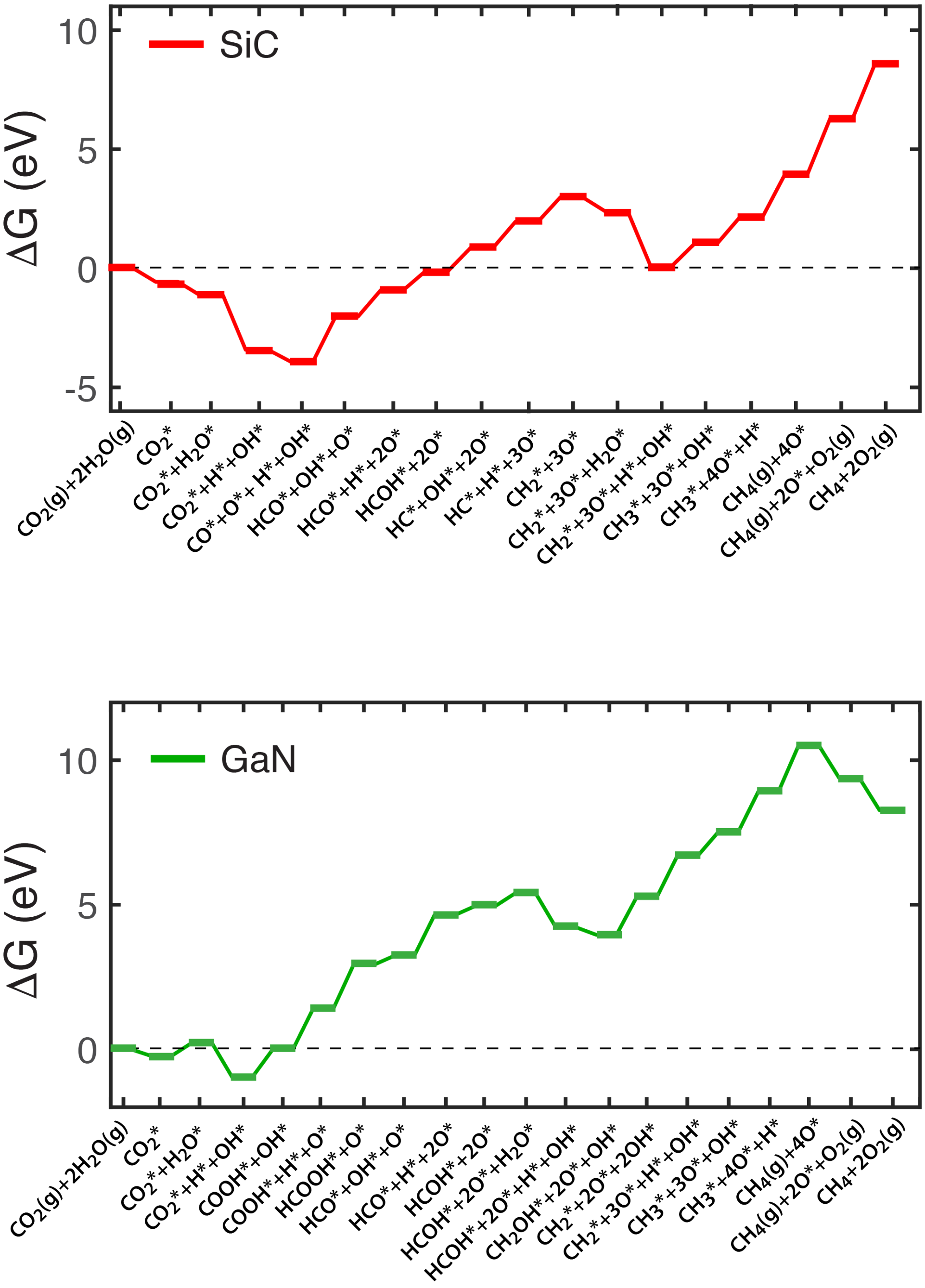

Figure S3: The reaction energetics with stoichiometrically balanced species for CO_2 reduction over SiC (top) and GaN (bottom) towards CH_4 production via ab initio thermodynamics approach (T = 350 °C and ambient pressure). Redox and carboxylic routes were isolated as most favorable pathways for the initiation of CO_2 reduction over SiC and GaN, respectively.

3.2. Other Reaction Pathways

Beyond the lowest energy reaction pathways discussed already, other reaction pathways close in energy may also be active under the range of reaction conditions considered herein (1.5 AM to concentrated illumination and ambient to elevated temperatures). Over GaN, 1st C–O cleavage via the formic route (CO_2* to form HCO_2*, $\Delta E = +1.71$ eV and $E_a = 2.88$ eV) was found closest in energy yet less favorable than the isolated most favorable carboxylic pathway via COOH* intermediate (endothermic by $\Delta E = +0.89$ eV and $E_a = 1.56$ eV). Similarly, after first C–O cleavage over GaN, hydrogenation of HCO* via formic-like route to form H_2CO* ($\Delta E = +1.12$ eV and $E_a = 2.01$ eV) was found closest in energy but less favorable than hydrogenation of HCO* intermediate via carboxylic route to HCOH* ($\Delta E = +0.18$ eV, $E_a = 0.30$ eV).

Over SiC, reaction pathways closest to the minimum energy redox pathway isolated were less thermodynamically favorable by at least 2 eV and exhibited significantly larger kinetic barriers. Hydrogenation of CO_2* via carboxylic route (COOH*) and formic route (HCO_2*) were both less energetically favorable ($\Delta E = +1.80$ eV and $E_a = 2.66$ eV , and $\Delta E = +1.65$ eV and $E_a = 2.80$ eV, respectively). After the formation of CO*, direct dissociation via redox route to form C* was close in energy ($\Delta E = +2.03$ eV and $E_a = 3.10$ eV), yet less favorable than hydrogenation of CO* via formic route ($\Delta E = +1.19$ eV and $E_a = 2.16$ eV). Despite the elevated energy requirements for these pathways, they may contribute to the observed catalytic activity and product distributions depending upon how the energy of the absorbed photon is partitioned between electrochemical redox reaction steps and vibrational excitation of surface-bound reaction intermediates through non-radiative excited electron energy dissipation.

All reaction pathways calculated to isolate the most energetically favorable reaction mechanism have been included in Figures S4-S12 and S13-S21 over SiC and GaN, respectively. Kinetic barriers for reaction steps with thermodynamic energetics greater than 3.2 eV were not calculated since the barrier energetics can be assumed to be much higher than thermodynamic energetics and these pathways will likely not contribute to the overall activity and product distribution.

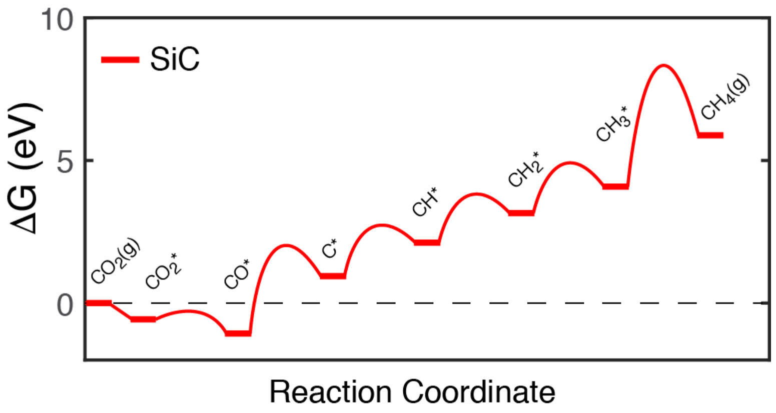

Figure S4: Less favorable surface reaction pathway #2 calculated for CO_2 reduction over SiC towards CH_4 production via ab initio thermodynamics approach (T = 350 °C and ambient pressure). Redox and carboxylic routes, isolated as most favorable pathways for the initiation of CO_2 reduction over SiC and GaN, respectively, are shown in main document Figure 3.

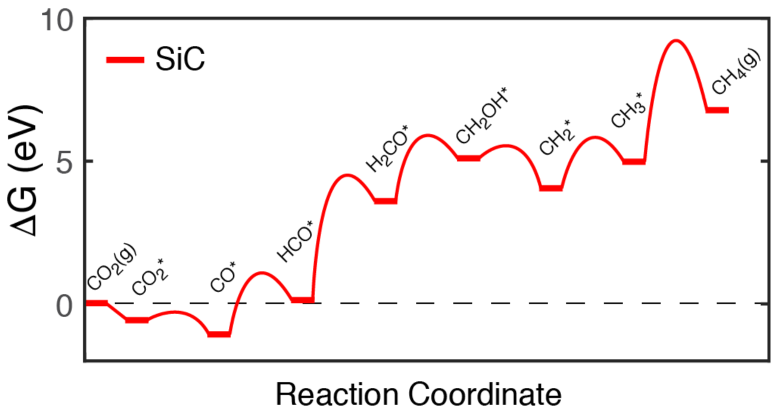

Figure S5: Less favorable surface reaction pathway #3 calculated for CO_2 reduction over SiC towards CH_4 production via ab initio thermodynamics approach (T = 350 °C and ambient pressure). Redox and carboxylic routes, isolated as most favorable pathways for the initiation of CO_2 reduction over SiC and GaN, respectively, are shown in main document Figure 3.

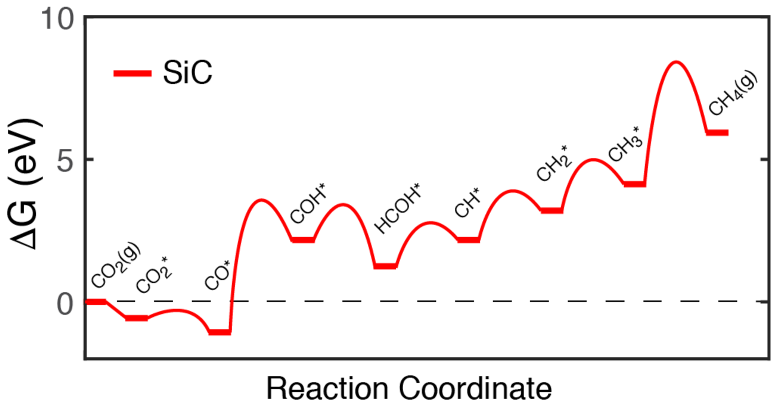

Figure S6: Less favorable surface reaction pathway #4 calculated for CO_2 reduction over SiC towards CH_4 production via ab initio thermodynamics approach (T = 350 °C and ambient pressure). Redox and carboxylic routes, isolated as most favorable pathways for the initiation of CO_2 reduction over SiC and GaN, respectively, are shown in main document Figure 3.

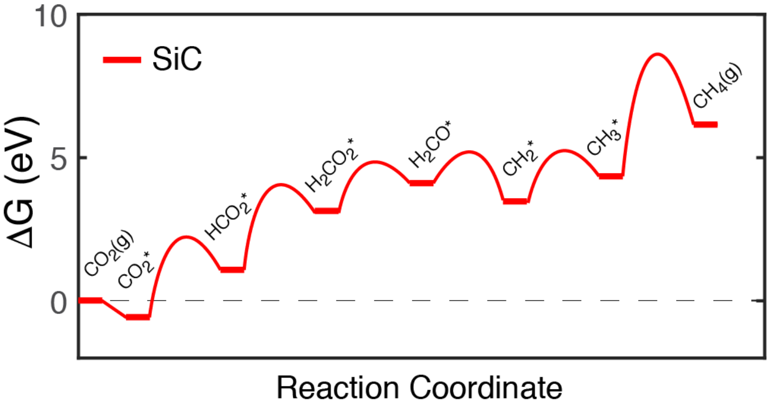

Figure S7: Less favorable surface reaction pathway #5 calculated for CO_2 reduction over SiC towards CH_4 production via ab initio thermodynamics approach (T = 350 °C and ambient pressure). Redox and carboxylic routes, isolated as most favorable pathways for the initiation of CO_2 reduction over SiC and GaN, respectively, are shown in main document Figure 3.

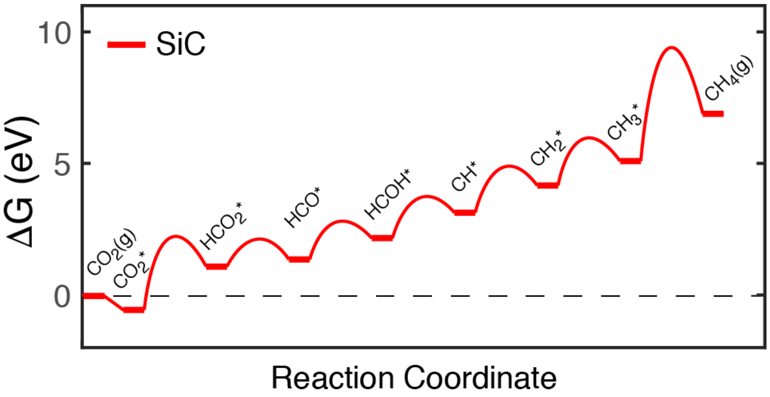

Figure S8: Less favorable surface reaction pathway #6 calculated for CO_2 reduction over SiC towards CH_4 production via ab initio thermodynamics approach (T = 350 °C and ambient pressure). Redox and carboxylic routes, isolated as most favorable pathways for the initiation of CO_2 reduction over SiC and GaN, respectively, are shown in main document Figure 3.

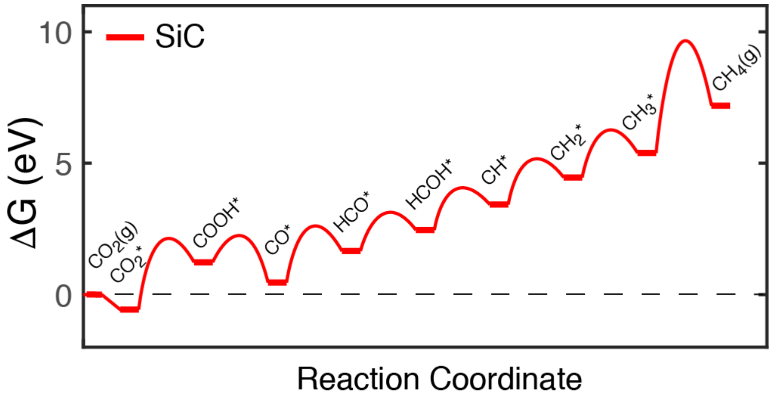

Figure S9: Less favorable surface reaction pathway #7 calculated for CO_2 reduction over SiC towards CH_4 production via ab initio thermodynamics approach (T = 350 °C and ambient pressure). Redox and carboxylic routes, isolated as most favorable pathways for the initiation of CO_2 reduction over SiC and GaN, respectively, are shown in main document Figure 3.

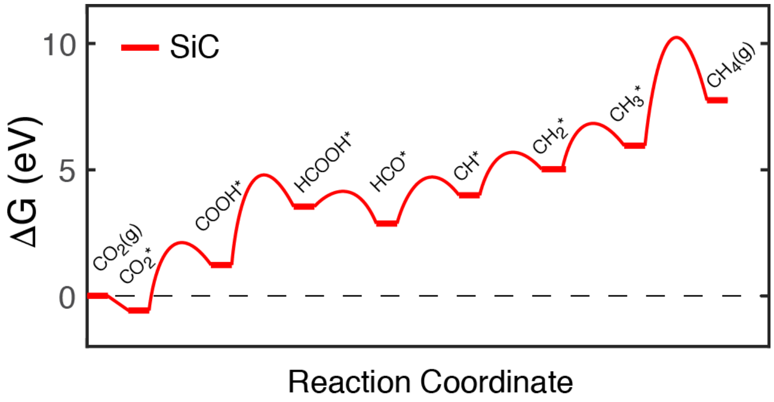

Figure S10: Less favorable surface reaction pathway #8 calculated for CO_2 reduction over SiC towards CH_4 production via ab initio thermodynamics approach (T = 350 °C and ambient pressure). Redox and carboxylic routes, isolated as most favorable pathways for the initiation of CO_2 reduction over SiC and GaN, respectively, are shown in main document Figure 3.

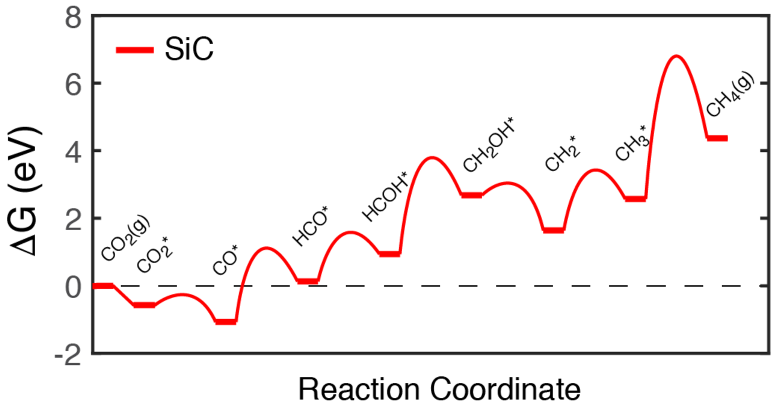

Figure S11: Less favorable surface reaction pathway #9 calculated for CO_2 reduction over SiC towards CH_4 production via ab initio thermodynamics approach (T = 350 °C and ambient pressure). Redox and carboxylic routes, isolated as most favorable pathways for the initiation of CO_2 reduction over SiC and GaN, respectively, are shown in main document Figure 3.

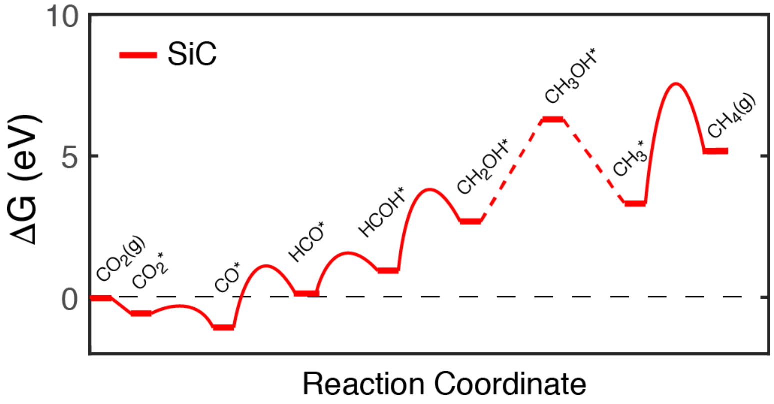

Figure S12: Less favorable surface reaction pathway #10 calculated for CO_2 reduction over SiC towards CH_4 production via ab initio thermodynamics approach (T = 350 °C and ambient pressure). Dashed lines are shown for highly energetic reaction steps whose kinetic barriers were not calculated. Redox and carboxylic routes, isolated as most favorable pathways for the initiation of CO_2 reduction over SiC and GaN, respectively, are shown in main document Figure 3.

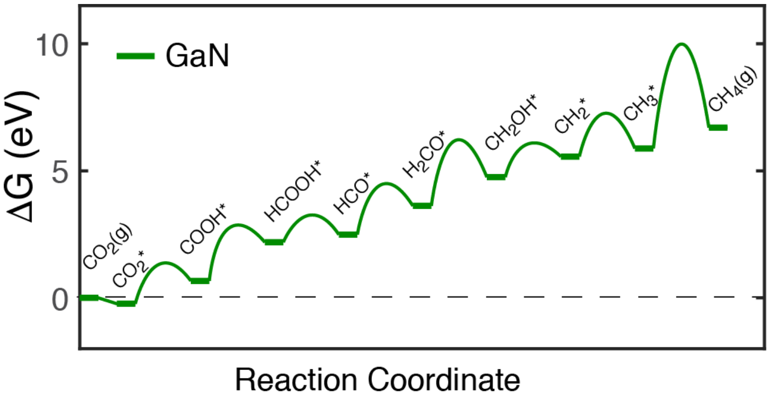

Figure S13: Less favorable surface reaction pathway #2 calculated for CO_2 reduction over GaN towards CH_4 production via ab initio thermodynamics approach (T = 350 °C and ambient pressure). Redox and carboxylic routes, isolated as most favorable pathways for the initiation of CO_2 reduction over SiC and GaN, respectively, are shown in main document Figure 3.

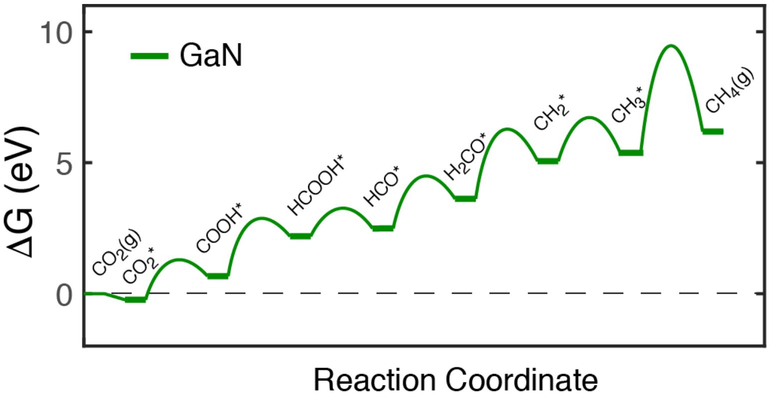

Figure S14: Less favorable surface reaction pathway #3 calculated for CO_2 reduction over GaN towards CH_4 production via ab initio thermodynamics approach (T = 350 °C and ambient pressure). Redox and carboxylic routes, isolated as most favorable pathways for the initiation of CO_2 reduction over SiC and GaN, respectively, are shown in main document Figure 3.

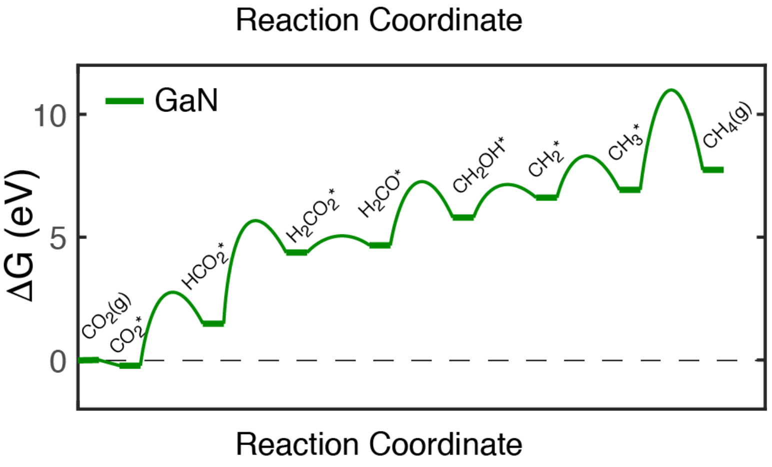

Figure S15: Less favorable surface reaction pathway #4 calculated for CO_2 reduction over GaN towards CH_4 production via ab initio thermodynamics approach (T = 350 °C and ambient pressure). Redox and carboxylic routes, isolated as most favorable pathways for the initiation of CO_2 reduction over SiC and GaN, respectively, are shown in main document Figure 3.

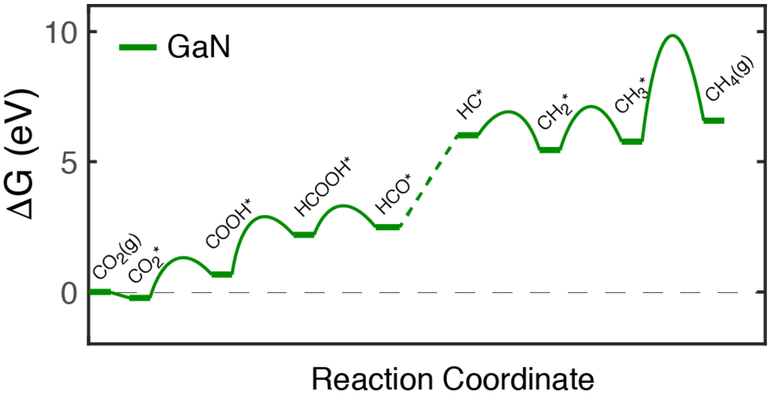

Figure S16: Less favorable surface reaction pathway #5 calculated for CO_2 reduction over GaN towards CH_4 production via ab initio thermodynamics approach (T = 350 °C and ambient pressure). Dashed lines are shown for highly energetic reaction steps whose kinetic barriers were not calculated. Redox and carboxylic routes, isolated as most favorable pathways for the initiation of CO_2 reduction over SiC and GaN, respectively, are shown in main document Figure 3.

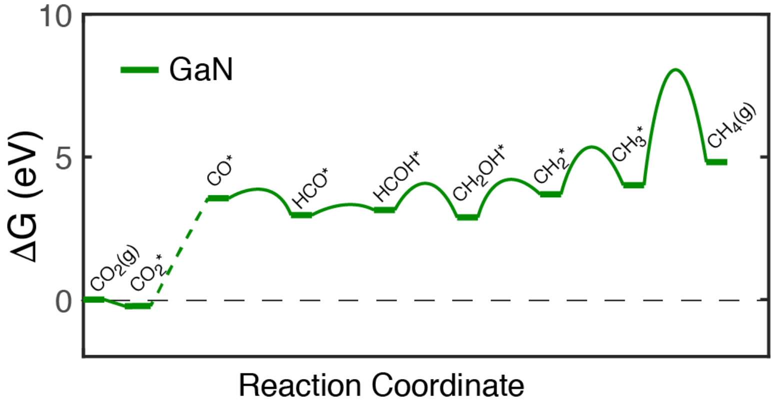

Figure S17: Less favorable surface reaction pathway #6 calculated for CO_2 reduction over GaN towards CH_4 production via ab initio thermodynamics approach (T = 350 °C and ambient pressure). Dashed lines are shown for highly energetic reaction steps whose kinetic barriers were not calculated. Redox and carboxylic routes, isolated as most favorable pathways for the initiation of CO_2 reduction over SiC and GaN, respectively, are shown in main document Figure 3.

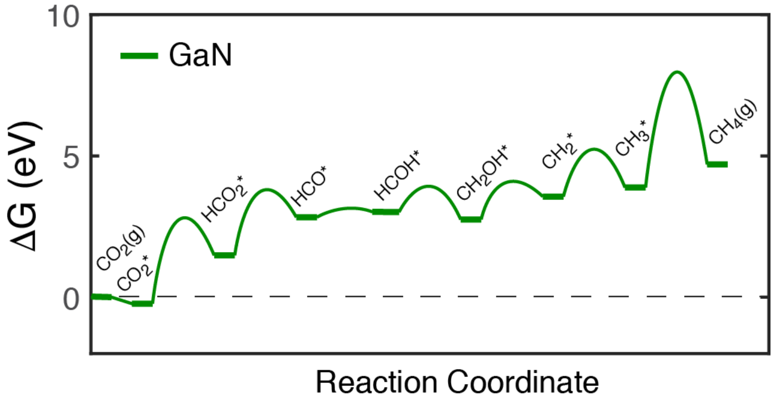

Figure S18: Less favorable surface reaction pathway #7 calculated for CO_2 reduction over GaN towards CH_4 production via ab initio thermodynamics approach (T = 350 °C and ambient pressure). Redox and carboxylic routes, isolated as most favorable pathways for the initiation of CO_2 reduction over SiC and GaN, respectively, are shown in main document Figure 3.

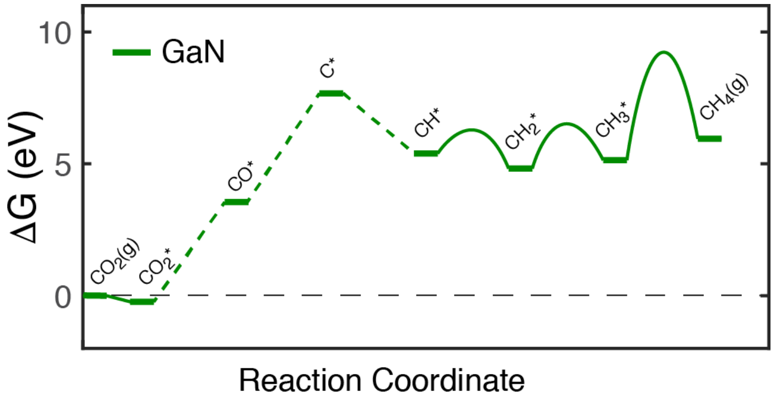

Figure S19: Less favorable surface reaction pathway #8 calculated for CO_2 reduction over GaN towards CH_4 production via ab initio thermodynamics approach (T = 350 °C and ambient pressure). Dashed lines are shown for highly energetic reaction steps whose kinetic barriers were not calculated. Redox and carboxylic routes, isolated as most favorable pathways for the initiation of CO_2 reduction over SiC and GaN, respectively, are shown in main document Figure 3.

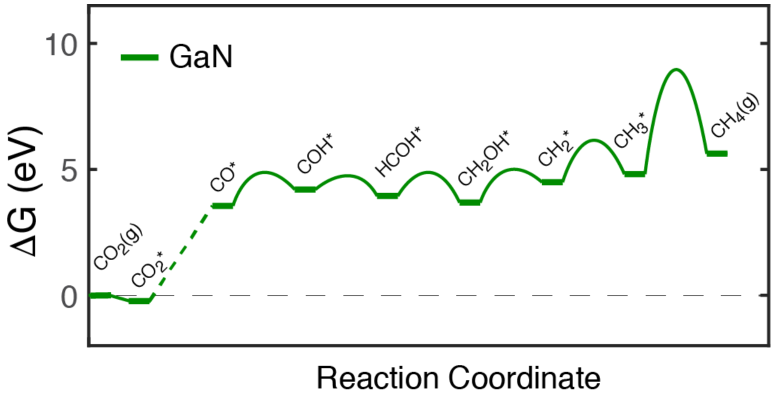

Figure S20: Less favorable surface reaction pathway #9 calculated for CO_2 reduction over GaN towards CH_4 production via ab initio thermodynamics approach (T = 350 °C and ambient pressure). Dashed lines are shown for highly energetic reaction steps whose kinetic barriers were not calculated. Redox and carboxylic routes, isolated as most favorable pathways for the initiation of CO_2 reduction over SiC and GaN, respectively, are shown in main document Figure 3.

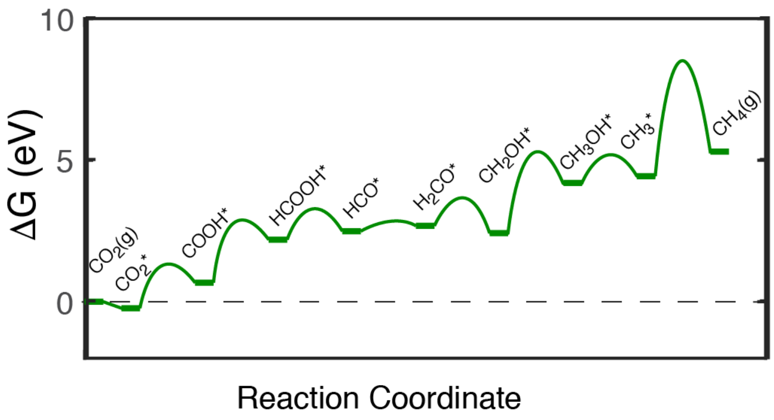

Figure S21: Less favorable surface reaction pathway #10 calculated for CO_2 reduction over GaN towards CH_4 production via ab initio thermodynamics approach (T = 350 °C and ambient pressure). Redox and carboxylic routes, isolated as most favorable pathways for the initiation of CO_2 reduction over SiC and GaN, respectively, are shown in main document Figure 3.

3.3. Molecular and Dissociative Adsorption Energies(eV)

Table S1: Dissociative adsorption energies of H_2, O_2, H_2O, and CO_2, and molecular adsorption of CO over SiC and GaN surfaces with respect to the energies of molecular sources. Negative and positive adsorption energies indicate exothermic and endothermic energies of adsorption, respectively. Results suggest that all probe molecules adsorb molecularly or dissociatively more favorably over SiC compared to GaN.

Catalyst	H_2 diss	O_2 diss	H_2O diss	CO_2 diss	CO ads
SiC	-2.5	-1.8	-2.3	-0.5	-2.4
GaN	-0.7	-0.1	-1.3	+3.7	-0.1

Table S2: Dissociative adsorption energies of H_2, O_2, H_2O, and molecular adsorption of CO over pristine SiC and partially oxidized SiC_xO_y (11% oxidized) surfaces with respect to the energies of molecular sources. Negative and positive adsorption energies indicate exothermic and endothermic energies of adsorption, respectively. Results suggest that all probe molecules, except H_2O, adsorb molecularly or dissociatively more favorably over pristine SiC compared to SiC_xO_y surface.

Catalyst	H_2 diss	O_2 diss	H_2O diss	CO ads
SiC	-2.50	-1.81	-2.26	-2.48
SiC_xO_y	-2.13	-1.09	-2.37	-1.52

3.4. Relative Stability(eV)

Table S3: Relative stability of key reaction intermediates encountered in the CO_2 reduction pathway towards CH_4 formation, calculated by subtracting adsorption energies over SiC from adsorption energies over GaN. Note that positive stability values mean less stable. Results suggest that key intermediates are relatively stabilized over SiC, by at least 0.9 eV.

Catalyst	CH*	CH_2*	CH_3*	HCO*	C*	COOH*
Relative stability (E_{GaN}-E_{SiC})	2.0	1.4	2.3	0.9	2.7	1.1

Table S4: Relative stability of a few key reaction intermediates encountered in the CO_2 reduction pathway towards CH_4 formation, calculated by subtracting adsorption energies over partially oxidized SiC surface (11% oxidized) from adsorption energies over pristine SiC surface. Note that positive stability values mean less stable. Results suggest that key intermediates are relatively stabilized over SiC, except the CH3* intermediate

Catalyst	CH*	CH_2*	CH_3*	C*
Relative stability (E_{SiCxOy}-E_{SiC})	1.53	0.73	-1.80	1.56

4. Calculation Files

The INCAR files utilized in calculations of thermodynamic energetics and kinetic barriers via cNEB or DIMER are provided below:

4.1. INCAR of a cNEB on GaN or SiC:

```
NWRITE = 2
ISTART = 0
ISPIN = 2
GGA = PS
NPAR = 16
NUPDOWN = 0
ENCUT = 400.0
EDIFF = 0.0001
LREAL = Auto
NELM = 60
NELMIN = 6
```

```
ALGO = FAST
EDIFFG = -0.1
IBRION = 3
IOPT = 3
NSW = 3000
NBLOCK = 1
ISMEAR = 0
SIGMA = 0.05
POTIM = 0.0
IDIPOL = 3
LDIPOL = .TRUE.
ICHAIN = 0
IMAGES = 9
SPRING = -5
LCLIMB = TRUE.
```

4.2. INCAR of thermodynamic calculation over SiC or GaN:

```
NWRITE = 2
ISTART = 0
ISPIN = 2
GGA = PS
NPAR = 16
NUPDOWN = 0
ENCUT = 400.0
EDIFF = 0.0001
LREAL = Auto
NELM = 60
NELMIN = 6
EDIFFG = -0.1
IBRION = 2
NSW = 300
NBLOCK = 1
ALGO = FAST
ISMEAR = 0
SIGMA = 0.05
POTIM = 0.01
```

```
IDIPOL = 3
LDIPOL = .TRUE.
```

4.3. INCAR of DIMER calculation over SiC or GaN:

```
IBRION=3
POTIM=0.0
ISYM=0
NSW=3000
EDIFF=1E-7
EDIFFG=-0.001
PREC=Norm
LREAL=.FALSE.
LWAVE=.FALSE.
LCHARG=.FALSE.
GGA=PS
NWRITE=2
ISTART=0
ISPIN=1
ISMEAR=0
SIGMA=0.05
NELM=60
NELMIN=6
ICHAIN=2
DdR=0.005
DRotMax=4
DFNMin=0.01
DFNMax=1.0
IOPT=2
IDIPOL = 3
LDIPOL = .TRUE.
```

5. References

[1] K. Reuter and M. Scheffler, *Physical Review B*, 2001, **65**, year.

[2] J. Rogal, K. Reuter and M. Scheffler, *Physical Review B*, 2007, **75**, year.